University of Plymouth

PEARL **https://pearl.plymouth.ac.uk**

Faculty of Science and Engineering School of Biological and Marine Sciences

1997-12-15

Capture and release of Lagrangian floats by eddies in shear flow

Shapiro, Georgy

http://hdl.handle.net/10026.1/9738

10.1029/97jc02386
Journal of Geophysical Research: Oceans
American Geophysical Union (AGU)

All content in PEARL is protected by copyright law. Author manuscripts are made available in accordance with publisher policies. Please cite only the published version using the details provided on the item record or document. In the absence of an open licence (e.g. Creative Commons), permissions for further reuse of content should be sought from the publisher or author.

JOURNAL OF GEOPHYSICAL RESEARCH, VOL. 102, NO. C13, PAGES 27,887–27,902, DECEMBER 15, 1997

Capture and release of Lagrangian floats by eddies in shear flow

G. I. Shapiro

P. P. Shirshov Institute of Oceanology, Russian Academy of Sciences, Moscow

E. D. Barton

School of Ocean Sciences, University College of North Wales, Anglesey

S. L. Meschanov

P. P. Shirshov Institute of Oceanology, Russian Academy of Sciences, Moscow

Abstract. A mechanism to explain the observed trapping or release of Lagrangian drifters by eddies is proposed, based on an interaction between the eddy circulation and the background flow. Eddies strong in relation to the background have a large "trap zone" within which particles are constrained to circulate in closed paths about the center, while relatively weak eddies have a smaller trap zone. Particles outside the trap zone drift freely, while those inside rotate with the eddy. As an eddy is advected by non-uniform shear flow, its 'trap zone' expands or contracts so particles previously free become trapped or trapped particles are freed. Numerical experiments with idealized eddies embedded in different flows illustrate the concept. It is shown that drifters may begin to loop, as in some previously reported observations, without any need for eddy generation. Similarly, they may cease looping, without eddy destruction. The particular case of a strong cyclonic eddy south of Gran Canaria is modeled, using the observed density field and two drifter trajectories. Predicted drifter trajectories are compared with the observations. It is shown that the trajectories of buoys launched near the edge of the eddy are sensitive to small variations in the background field.

1. Introduction

Observations of ocean currents with drifting Lagrangian buoys (surface drifters or neutral buoyancy floats) have become increasingly common and complement traditional Eulerian observations made at a fixed location [see, e.g., *Kirwan*, 1988, *Richardson et al.*, 1989, *Pingree and Le Cann*, 1991, *Zenk et al*, 1992, *Schultz Tokos et al.*, 1994, *Sanderson*, 1995, *Bower et al.*, 1995 and references therein]. In general, the interpretation of Lagrangian properties from an Eulerian point of view and vice versa is not always obvious and needs particular care. It is known that differences between Lagrangian and Eulerian current velocity measurements from drifters and nearby moorings are in part due to the inherent difference between the spatial and temporal averaging of discrete data. An example was provided by *Kirwan* [1988] who showed that the flow center of mesoscale eddies is not generally coincident with the center obtained by averaging the positions of all drifters at some instant .

Numerous observations of mesoscale and synoptic scale eddies with Lagrangian drifters show that while some buoys remain trapped in eddies for long periods, other buoys abruptly cease their rotatory motion and drift away [see, e.g., *Gründlingh*, 1978, *Cheney et al.*, 1980, *Pingree and Le Cann*, 1991, *Sanderson*, 1995]. A theoretical explanation based on the integrated effects of windage and surface currents on an imperfectly drogued buoy was suggested by *Kirwan et al.* [1975] and *Pingree and Le Cann* [1991]. Their theoretical calculations and field tests show that this mechanism can account for the "blowing out" of a drogued buoy from an eddy under certain environmental conditions. However, this mechanism does not explain why well-drogued surface drifters, not influenced significantly by wind stress, are also expelled from eddies, as was observed by *Sanderson* [1995] during his measurements of the structure of an eddy on Western Bank, Scotian Shelf. Fourteen drifters were deployed in a cluster with initial dimensions of about 10 km. Twelve of these 14 drifters remained essentially within the eddy, but two of the drifters were lost from the eddy. Detided trajectories of some of the drifters (Figure 1) demonstrate, that even when released very close to each other, they have absolutely different positions after 5-6 days of tracking.

A different physical mechanism is also required to explain why neutral buoyancy floats launched in Mediterranean Eddies (Meddies) at a depth of several hundred meters can be lost quickly or remain inside for years [*Richardson et al.*, 1989]. Observations by *Bower et al.* [1995] show that two of five floats (AM116a and AM105) deployed into the Mediterranean Undercurrent in the Gulf of Cadiz made one or two anticyclonic loops around meddies but did not remain with the Meddies and drifted off. The interaction between two adjacent meddies was observed by *Schultz Tokos et al.* [1994] using

Copyright 1997 by the American Geophysical Union

Paper number 97JC02386.
0148-0227/97/97JC-023862$09.00

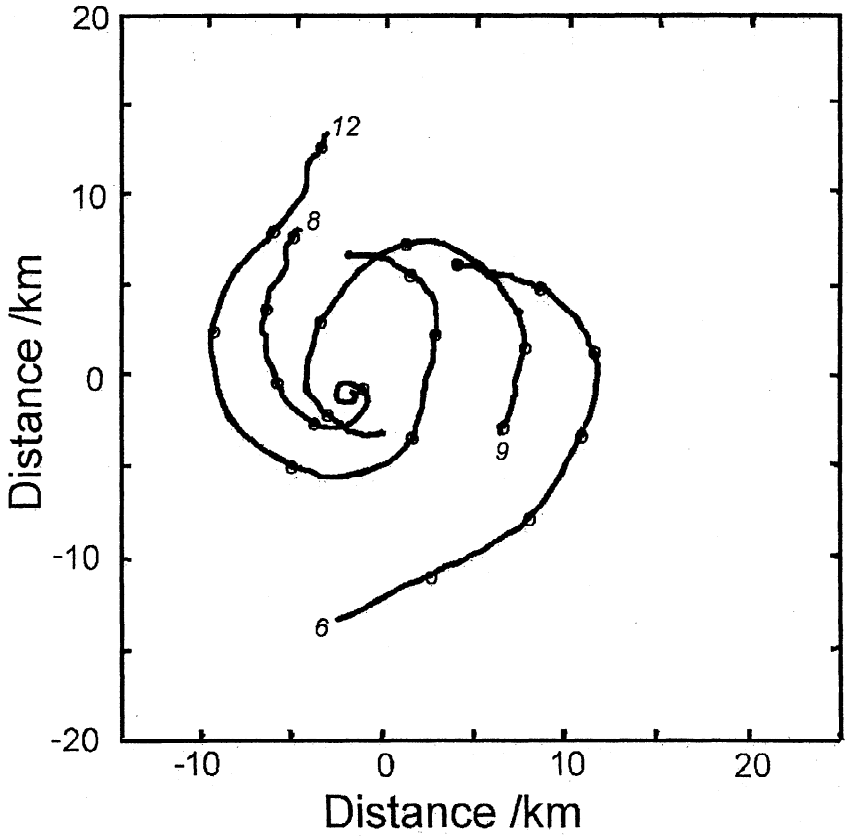

Figure 1. Detided trajectories for 4 of 14 drifters in an eddy on Western Bank, Scotian Shelf (reproduced from *Sanderson* [1995]).

four neutrally buoyant floats. The floats all made at least one revolution around the first meddy, and then, at various times, they left it and joined the closed circulation of the second meddy.

In this paper, a physical mechanism to explain both release and capture of Lagrangian floats by intensive vortices is proposed and discussed. This mechanism takes into account the balance between the eddy and background flow fields and can be applied to both near-surface and deep eddies. We pay special attention to the situation when an eddy is embedded in a background shear flow strong enough to influence the velocity structure of the eddy.

The mechanism is formulated and illustrated with some kinematic examples in section 2. Its efficiency is checked by a dynamic model for an idealized circular eddy in section 3. Examples are provided to show both "capture" and "expulsion" of the buoy. Then, in section 4 the dynamics and Lagrangian properties of a real eddy observed in the Canary basin are simulated. Field data gathered in August 1993 during the Hesperides Cruise 9308 in the framework of MAST-1 project 0031 define the background flow field and drifter trajectories associated with a pair of counter-rotating eddies. A generalized near-geostrophic equation (GNE) on the β-plane [*Shapiro*, 1986] is used to model the situation. The discussion and conclusions are found in section 5.

2. Concept and Kinematics

The pattern of oceanic flow is usually described in two ways. The first is the Eulerian approach that describes the velocity of the fluid at a selection of fixed points, for example, using information from anchored current meters. The second is the Lagrangian approach, that considers paths of fluid particles, for example, using data obtained from drifting floats. In principle, both ways are equivalent if one has complete information, which would require an infinite number of current meters and floats. In a more practical case of limited information the transition between the two descriptions may be far less obvious and sensitive to the accuracy of available data. Numerical models are usually based on an Eulerian framework, and any Lagrangian properties are derived indirectly from the calculated time-dependent Eulerian velocity fields [*Dewar and Flierl*, 1985, *Holloway et al.*, 1986]. Conversely, the estimation of Eulerian properties of the flow from observed Lagrangian tracks sometimes encounter considerable difficulty [*Kirwan*, 1988, *Sanderson et al*, 1995]. The combining of Eulerian and Lagrangian characteristics of flow is most problematical in regions with developed mesoscale structure, when currents are changing significantly with time and space.

In a steady state flow the Eulerian boundary of an eddy is defined as the position of the last closed streamline, or separatrix, in a coordinate system attached to the eddy. In the absence of any background flow the boundary could be indefinitely far as is the case for a Gaussian or a point vortex. In the presence of a background flow the separatrix exists if the eddy is strong compared to the background flow. Inside the area bounded by the separatrix ("trap zone") every streamline is closed. In a steady state flow, a streamline coincides with the trajectory of a Lagrangian particle, hence no particle could leave the trap zone. In a time varying flow, this is no longer the case since streamlines and Lagrangian trajectories do not now coincide.

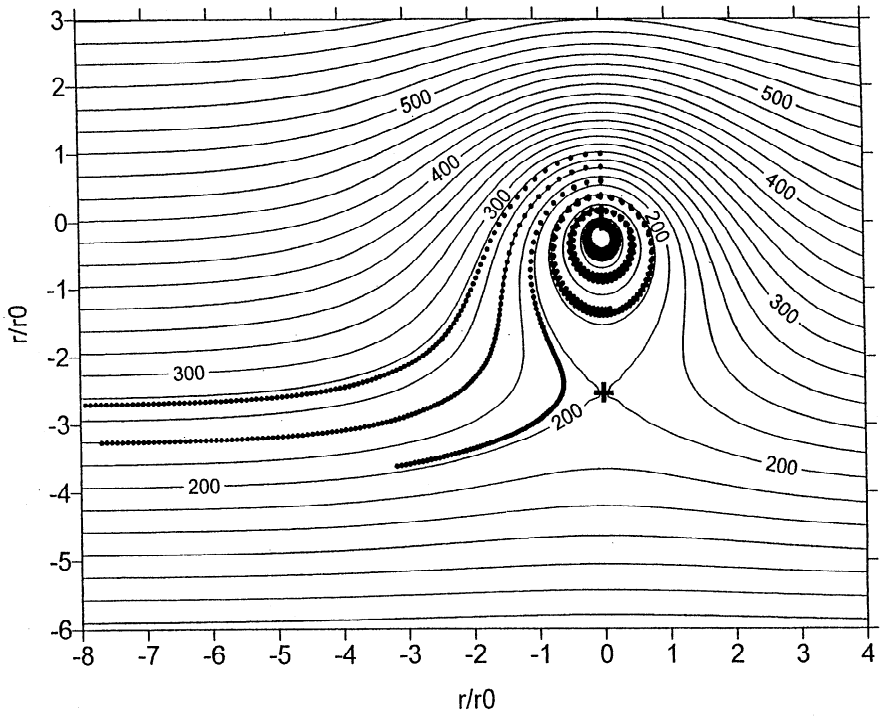

Figure 2. Streamlines (solid lines) of a circular vortex embedded in a uniform background flow U_0 for V_0/U_0=0.2. Trajectories (dotted lines) of six test floats with start points in the range $0<r<r_0$ are calculated by the Lagrangian block of the dynamical model. The coincidence between dotted and solid lines gives the idea of the accuracy of the Lagrangian block. Pluses show the vortex center and location of the stagnation point.

When the ratio of the eddy velocity to the background one changes (because of eddy decay, temporal or spatial variations of the background, or eddy acceleration/ deceleration), the area of the trap zone changes as well. As the background flow strengthens, the trap zone decreases and the separatrix moves toward the eddy center, crossing over fluid particles. A Lagrangian particle located originally inside the trap zone near the separatrix can find itself outside and so may drift away from the eddy. As the background flow weakens, the situation reverses, and a free moving particle could be incorporated into the eddy.

What is a likely mechanism that could change the ratio of eddy/background velocity? Intensive eddies are long-lived features, and their decay because of friction or lateral intrusions is a slow process and therefore acts on a longer timescale than relevant here. We hypothesize that the most probable mechanism is the advection of the eddy in a background flow featuring a spatially inhomogeneous horizontal shear. As the eddy is advected by the background flow to another location where the background velocity distribution differs from the original one, the trap zone changes its dimensions. The horizontal shear is an important feature of the proposed mechanism for eddies moving freely with the flow. In a spatially uniform steady flow a free eddy would be advected at the speed of the flow, and no changes in the trap zone would occur. A topographically arrested eddy, however, would experience temporal changes in the surrounding spatially uniform, but temporally variable, velocity field, and so the trap zone dimension would alter, even in the absence of shear.

To clarify the kinematics of this mechanism, consider an idealized circular eddy embedded in a surrounding flow. Assume that the distribution of absolute tangential velocity in the eddy is given by

$$V(r)= V_0\, r/r_0 \exp(-r/r_0), \qquad (1)$$

where $r=[(x-x_0)^2+(y-y_0)^2]$ corresponding to the Gaussian shape of the stream function. Here we consider a cyclonic eddy, but similar results are valid for an anticyclonic eddy. Equation (1) implies that the inner core of the eddy rotates counterclockwise approximately as a solid body with maximal velocity V_0 exp (-1) at distance r_0 from the center, and in an outer region the tangential velocity decreases with increasing radius.

Let the eddy be embedded in a uniform flow with velocity U_0, measured in the coordinate system attached to the eddy, directed along the x axis from right to left. Streamlines of the total flow and the boundaries of the trap zone are shown in Figure 2 for U_0/V_0= 0.2. This type of structure is well known, and illustrated, for example, by *Larichev and Reznik* [1976] and *Flierl* [1979]. More detailed calculation of the parameters of the separatrix for a Gaussian eddy for a variety of background fields can be found in papers by *Holloway et al.* [1986] and *Maksimenko and Orlov* [1991].

Examining this vortex-uniform flow combination, we find that there are two areas of different behavior of streamlines: in one area, where $V(r)>U_0$, streamlines are closed and near circular, whereas in the other area, where $V(r)<U_0$, streamlines are open. The distance R_0 between the original eddy center and the stagnation point on the separatrix can be found from the equation $V(R_0)=U_0$, or

$$\frac{R_0}{r_0}\exp\left(-\frac{R_0}{r_0}\right)=\frac{U_0}{V_0}. \qquad (2)$$

This distance is defined as the "trap zone radius of the eddy," although the actual area of the trap zone may not be circular.

It follows from (2) that for an eddy with fixed values of r_0 and V_0 the radius R_0 depends on the velocity U_0 of the background flow. The size of the trap zone decreases with an increase of U_0, and vanishes for intensive background flow with $U_0 > V_0 \exp(-1)$. For low U_0 values the trajectories of all particles launched within the eddy ($r/r_0<1$) are near circular and closed. As U_0 increases, the trajectories become increasingly open.

We consider this simple and well-known kinematic picture of a Gaussian eddy in uniform flow to make clear the hypothetical mechanism of float capture and release in a more complicated non steady shear background flow. The kinematic consideration itself is not a sufficient proof for the reality of the proposed mechanism as the transition between different kinematic patterns may or may not take place because of dynamical constraints. We consider the dynamical model in the next section.

3. Dynamics of Lagrangian Particles

Many types of mesoscale oceanic eddy, like meddies or surface eddies in the Canary basin, produce significant deviation of isopycnals from their equilibrium state. Because of this, the quasi-geostrophic equation is inadequate for study of the evolution and dynamics of these eddies. The geostrophic equations were extended to overcome this problem by *Williams* [1985], *Shapiro* [1986] and others. We use the "one-a-half layer" version of the generalized near-geostrophic equation (GNE) derived by *Shapiro* [1986]. In this model it is assumed that the real density stratification can be well approximated by a two-layered fluid, the lower layer being far deeper than the upper one. The GNE uses the "reduced gravity approximation" and has no restrictions on the amplitude of the isopycnal displacement. This equation filters out high-frequency gravity waves, as does the traditional quasi-geostrophic equation, and it includes some additional nonlinear terms.

We consider intense baroclinic eddies on a β plane (where $f=f_0+\beta y$ is the Coriolis parameter). In nondimensional variables, the GNE is written as [*Shapiro and Konshin*, 1989]

$$\frac{\partial H}{\partial t} - \nabla(1+\epsilon H)\nabla\frac{\partial H}{\partial t} = -J((1+\epsilon H)\nabla^2 H + \frac{1}{2}\epsilon|\nabla H|^2, H) + \frac{1+\epsilon H}{(1+\epsilon y)^2}\frac{\partial H}{\partial x} \qquad (3)$$

where

$$H(x,y,t)=\frac{h-h^*}{\epsilon h^*} \qquad (4)$$

and h are the nondimensional and dimensional, respectively, thickness of the dynamically active layer; h^*=const is its typical value; ∇ is the horizontal gradient operator; J is the Jacobian operator; $\epsilon=(\beta L_R)/f_0$ is the sphericity parameter; and $L_R=(g'h^*)^{1/2}/f_0$ is the internal radius of deformation. The horizontal distances and the time are nondimensionalized by the scales L_R and $(\beta L_R)^{-1}$, respectively. The parameter ϵ is assumed to be small on a β plane. At $\epsilon=0$, (4) reduces to the ordinary quasi-geostrophic potential vorticity equation. No external wind forcing is included, so only internal dynamical processes control the evolution of the flow field. A description of the finite difference scheme and numerical procedure of solution of (3) is given by *Shapiro and Konshin* [1989]. Because of the hydrostatic relation, $H(x,y)$ is proportional to the baroclinic pressure anomaly so that isolines of H show the pressure anomaly distribution.

The model is used for numerical simulation of the dynamics of the idealized eddy embedded in the variable shear flow $h(x,y)=h_v(x,y)+h_b(x,y)$, where h_v corresponds to the eddy and h_b to the background distribution

$$h_v(x,y)=-A_v\left(1+\frac{r}{r_0}\right)\exp\left(\frac{r}{r_0}\right), \qquad r=\sqrt{x^2+y^2}$$

$$G(\xi)=\left[\frac{1}{2}(\exp(\xi)+\exp(-\xi))\right]^{-4/3}$$

$$h_b(x,y)=A_h G\left(\frac{\sin\left(\frac{\pi y}{2y_{max}}\right)}{A_y G\left(A_x \sin\left(\frac{\pi x}{2x_{max}}\right)\right)}\right), \qquad (5)$$

and A_v, A_h, A_y, A_x, r_0 are constants and $2x_{max}$, $2y_{max}$ are the dimensions of the study area. A subregion of the initial distribution of $H(x,y)$ with $A_v = 30$, $A_h = 60$, $A_y = 98.4$, $A_x = 1.476$, $r_0 = L_R$ is shown in Figure 3a. In this example the strength of the shear of the background flow increases from left to right. Test float trajectories are indicated by heavy lines. Float A, released well within the trap zone, continues to rotate about the eddy, while float B outside it is carried downstream. Float C, released at an intermediate starting position within the trap zone but close to the separatrix, makes one cyclonic loop around the eddy and then drifts away. The behavior of float C relates to the motion of the eddy, which is indicated by the centers of the loops described by Float A. The eddy moved southwest then west into a region of stronger shear, so decreasing the trap zone and releasing the particle. This confirms that changes of background conditions around the eddy as it moves in the shear flow result in changes of the trap zone radius R_0. Floats initially trapped within the eddy and located near the separatrix can leave the eddy when it enters an area with more intensive shear (Figure 3a). In contrast, particles with starting points outside of the eddy trap zone can be incorporated into rotation around the eddy if the velocity of the background flow decreases as shown in Figure 3b. In this case, as the eddy moves southwest into weaker shear, its trap zone expands to capture the float initially located close outside the separatrix.

Figures 4a and b show the distribution of potential vorticity anomaly q corresponding to Figure 3a initially and after one of the floats has left the eddy. During the intervening period, the potential vorticity distribution has evolved so that the last closed isoline (separatrix contour value q=-26) opened. This allows the float to escape without any change in the potential vorticity of the water particle. The other float, placed initially closer to the center remained within the closed potential vorticity isolines area and continued to rotate about the eddy center.

The particular distribution of h given by (5) is not important. Numerical experiments with different eddy and background flow characteristics show similar behavior. The important considerations are (1) the relative strengths of the eddy and background flows and (2) the ability of the flow to advect the eddy to a location with noticeably different horizontal shear.

The above described behavior of floats in an idealized circular eddy moving in a shear flow is qualitatively similar to float trajectories observed in the Mediterranean Undercurrent

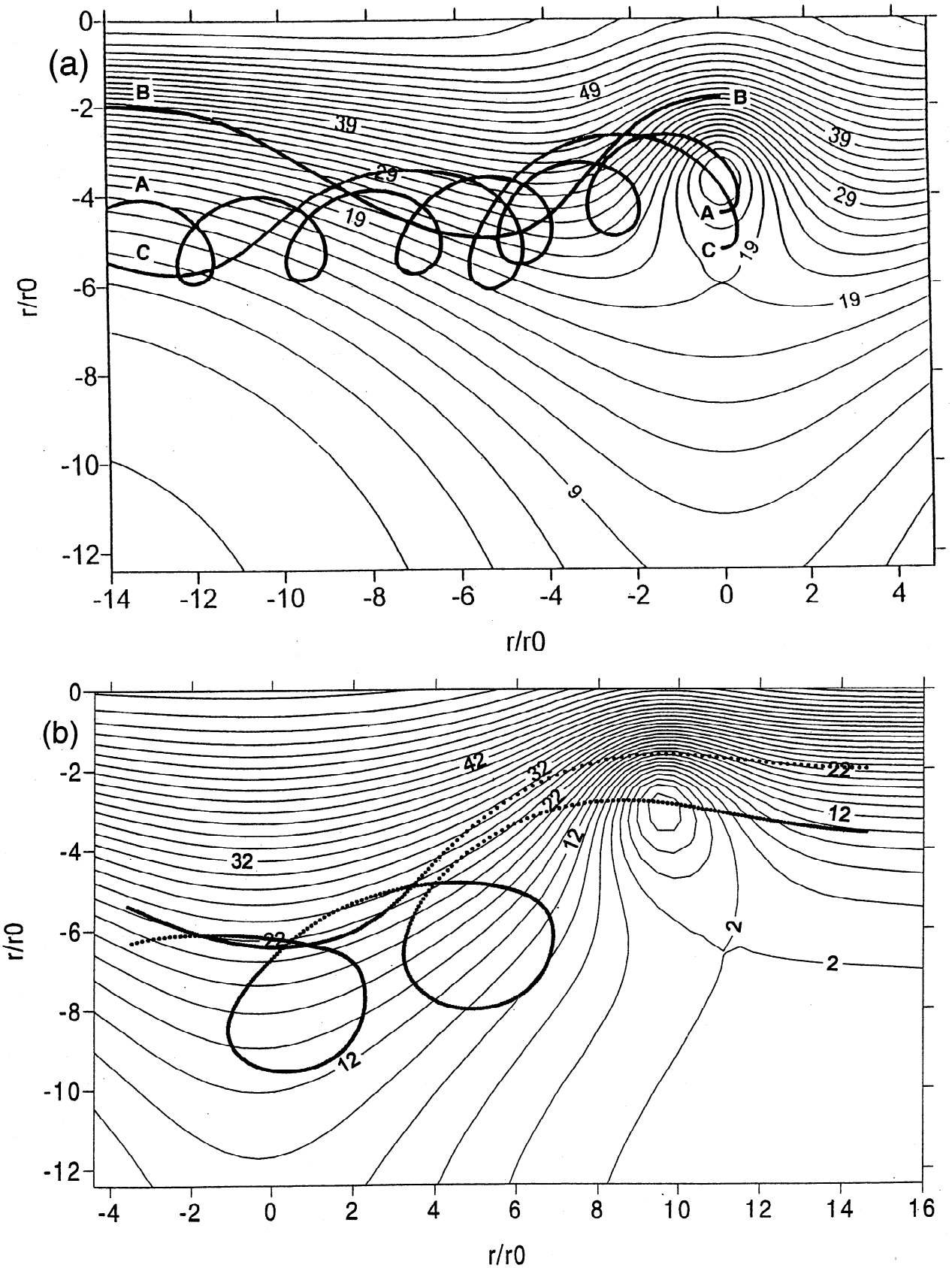

Figure 3. Initial streamline distributions and trajectories of Lagrangian floats calculated with the dynamical model for a circular eddy embedded in a shear flow. (a) The middle float A remains inside the eddy while the northernmost float B is at all times outside the trap zone; the float southernmost C is lost from the eddy after making one loop as the eddy moves into a region of stronger shear. (b) The southern float, which was originally free drifting, is caught by the eddy as its trap zone expands as the eddy moves into the region of lower background velocity. In both cases the eddy and background flow are the same; the only difference is their relative location.

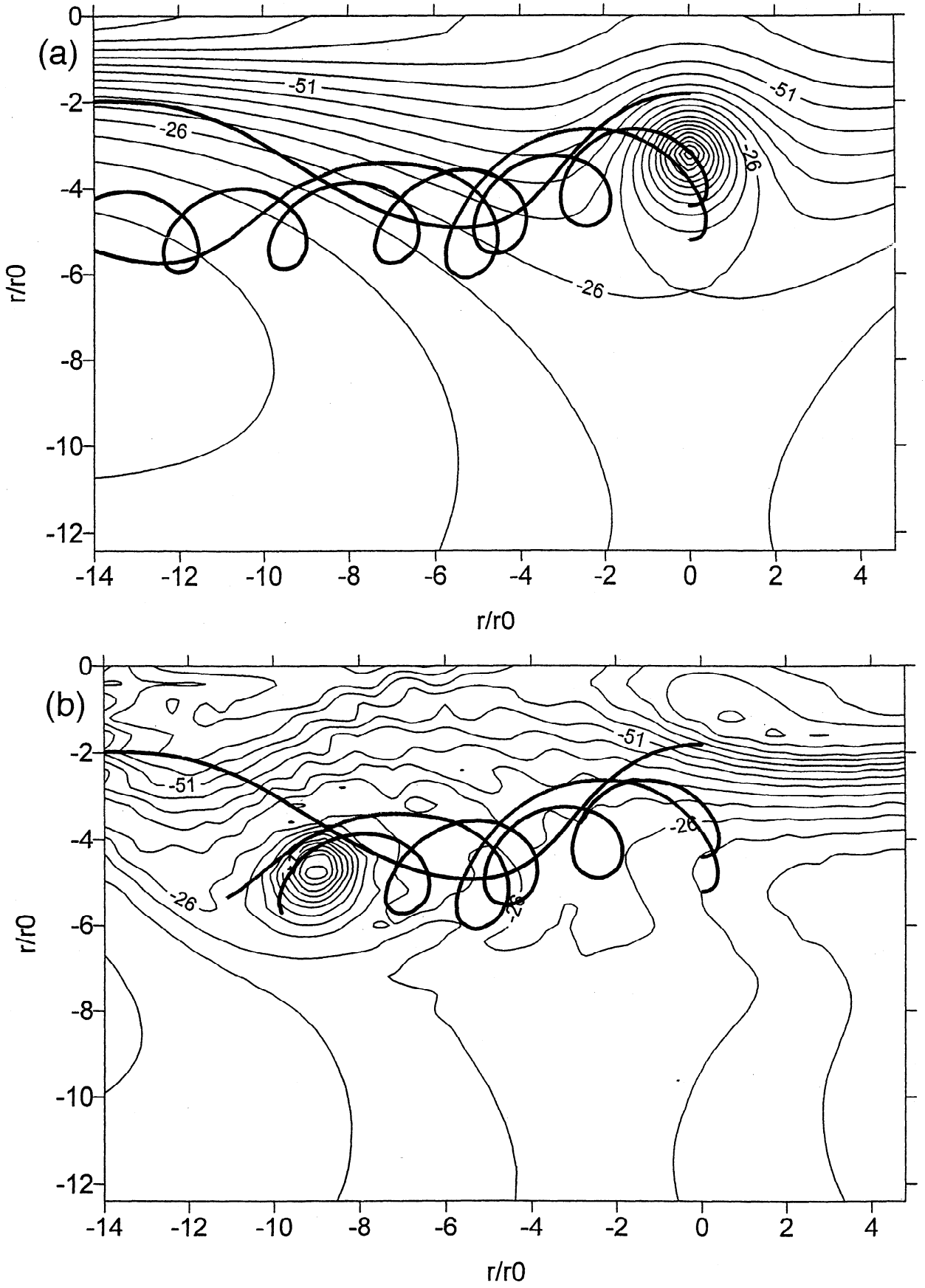

Figure 4. Distributions of potential vorticity anomaly corresponding to Figure 3a. (a) Initial distribution with complete float tracks. (b) Distribution at t=2.5 with portions of tracks up to then. Note the opening of the contour q=-26 which originally defined the separatrix has allowed the middle float to escape from the eddy without any change in its potential vorticity.

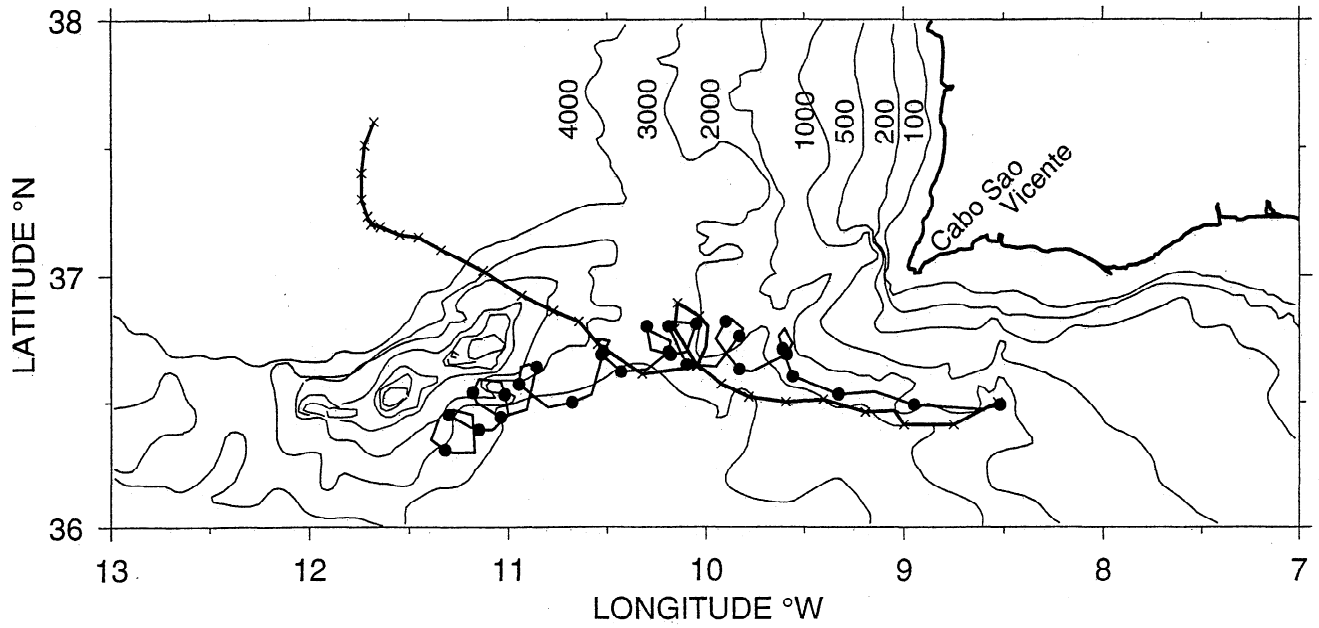

Figure 5. Trajectories of floats AM103 (circles) and AM105 (crosses) deployed 3 km apart in the Mediterranean Undercurrent [*Bower et al.*, 1995].

south of Portugal [*Bower et al.*, 1995]. Trajectories of floats AM103 (circles) and AM105 (crosses) deployed 3 km apart are shown in Figure 5. After about a week, the float AM103 was trapped in the core of a meddy and began a series of anticyclonic loops as the eddy moved southwestward. Float AM105 made only one anticyclonic loop around the same meddy, but then drifted off toward the northwest. The large radius of rotation (Figure 6) and quick departure of AM105 from the meddy suggest that it was initially just inside the trap zone but close to a separatrix line. Thus it circuited the eddy once but then was clearly outside the trap zone during the rest of its trajectory.

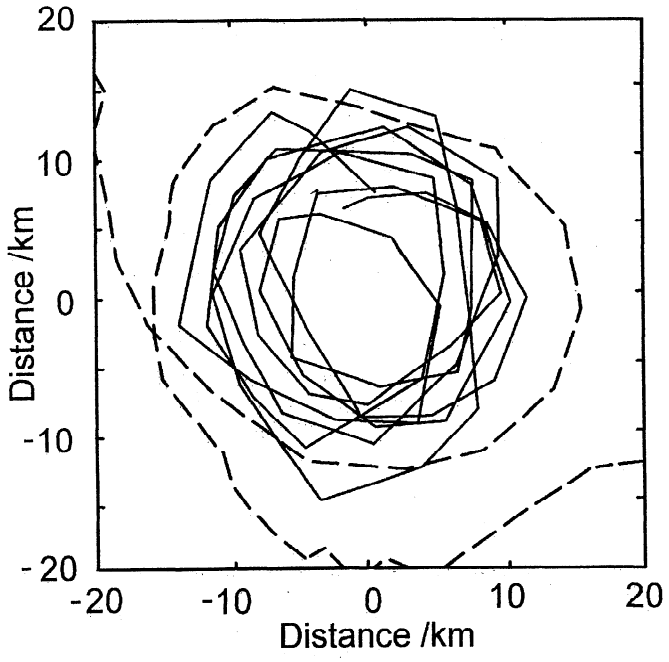

Figure 6. The motion of floats AM103 (solid) and AM105 (dashed) relative to the meddy center [*Bower et al.*, 1995].

4. Cyclonic Eddy South of Gran Canaria

The region to the south of Gran Canaria island is an eddy-rich area. Mesoscale eddies have been observed here repeatedly in 1990-1991 using satellite images and field measurements [*Arístegui et al.*, 1994, 1997]. The production of the eddies by Gran Canaria and the other islands contributes to enhanced mesoscale activity downstream [E.D. Barton, Eastern Boundary of the North Atlantic - Northwest Africa and Iberia, chapter submitted to *The Sea*, 1996]. The observations suggest that they are common mesoscale features in the flow past the Gran Canaria throughout the year. The eddies have a typical diameter of about 50 km and extend to several hundred meters depth.

In August 1993 a cyclonic eddy was identified southwest of Gran Canaria island (27.8°N, 16°W) from a satellite infrared image as a patch of water with relatively low sea surface temperature. A few days later the eddy was surveyed twice by the research vessel Hesperides using a SeaBird SBE-911 conductivity-temperature-depth (CTD) profiler with accuracy of 0.001°C and 0.001 psu for temperature and salinity, respectively [Navarro Pérez *et al.*, 1994]. Two Argos Data Collection and Location System satellite-tracked surface drifters were released with the aim of following the trajectory and velocity of the eddy. One of the drifters was released on the edge of the cyclonic eddy and the other in its center. The center of the eddy (stations with the lowest values of 50/500 m geopotential) was located at 27.30°N, 16.30°W during the first survey (August 19) and at 26.80°N, 16.50°W during the second one (24 August). Over the interval of five days between surveys the eddy drifted southwestwards at a speed of 0.14 m/s. CTD stations carried out to a depth of 500 m or greater during the first and second surveys (August 13-20 and 24-25, 1993) were used for the analysis of the eddy dynamics.

In order to get the initial distribution of the nondimensional depth of the upper layer $H(x,y)$ for numerical modeling, the observed CTD data were processed in several steps. First, the eddy drift velocity was used to adjust the location of stations carried out during the first survey to obtain a "synchronized"

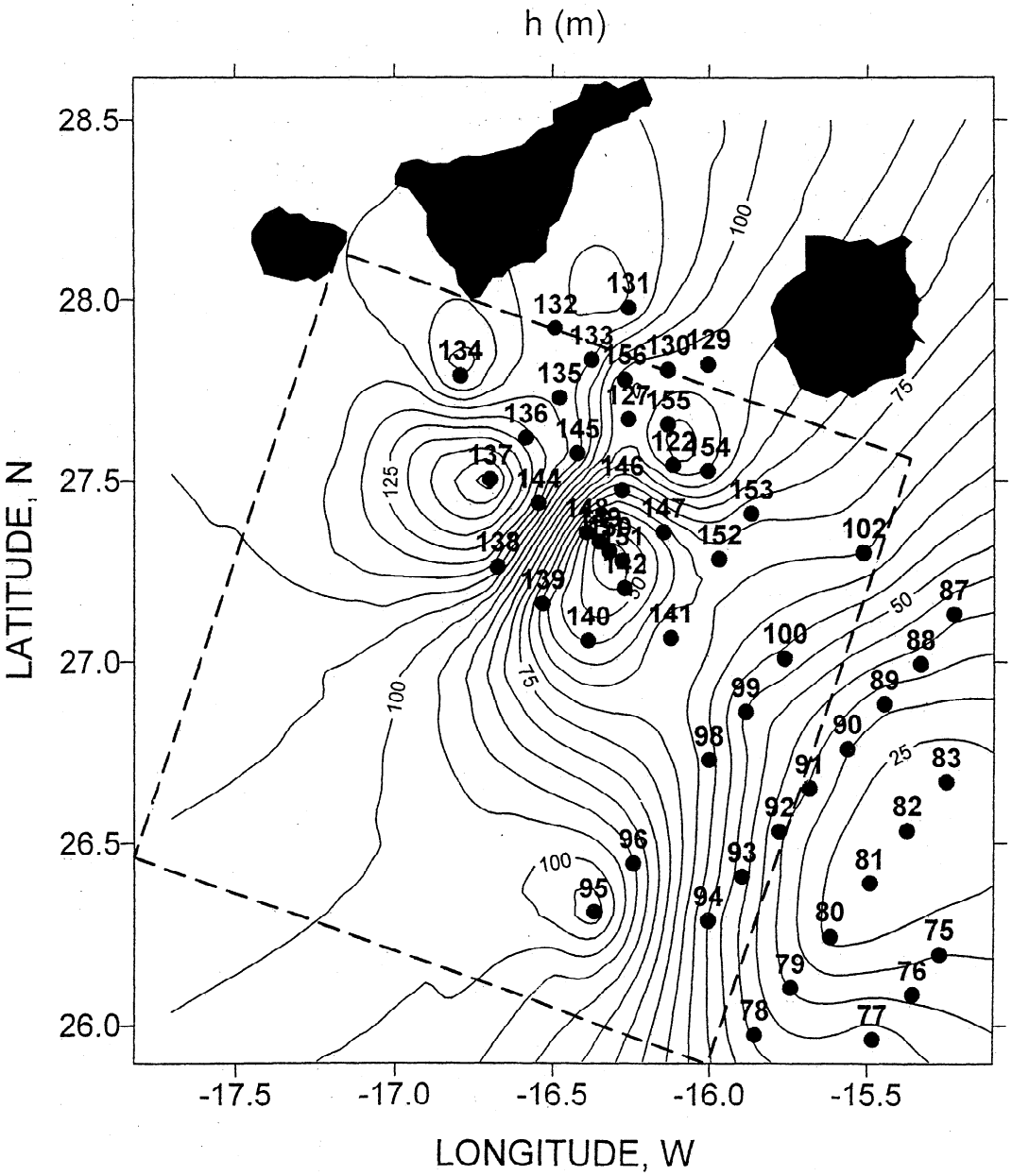

Figure 7. Locations of Hesperides CTD stations during the first survey of the eddy obtained after correction using (5). Dashed box indicates the area modeled for which results are shown in later figures.

pattern of hydrographic characteristics in the study area and take account of the advection of the water column during the survey:

$$\vec{r}'=\vec{r}+(t-t_0)\vec{V}, \tag{6}$$

where r' is the corrected location of a station; r and t are real location and time of a station, respectively; t_0 is the time of station carried out near the eddy center; V is the estimated velocity of the eddy displacement. This correction is small in the vicinity of the eddy, which was surveyed first, but amounts to adjustments of up to 30 km at the last stations at the southeastern corner of the survey area. Second, geopotential was computed based on an assumed level of no motion at 500 m. Values of geopotential at 50 m (x,y) were interpolated over the area 25.9-28.5°N, 15.1-17.7°W into the nodes of a rectangular grid of 40 x 40 points with nominal spatial resolution of 7.5 km in both directions. Third, the system of coordinates was rotated to direct the x axis along the line connecting the eddy centers in the first and second surveys.

The initial distribution of h and values of g', h^*, L_R are derived from a vertical section of observed density σ_θ across the eddy and surrounding water, and values of geopotential $\Phi(x,y)$ at the 50 m level with respect to 500 m using a two-stage procedure.

The reduced gravity for a two-layer ocean is defined as $g'=g(\rho_2-\rho_1)/\rho_2$, where the densities of upper ρ_1 and lower ρ_2 layers are assumed constant. When reducing the stratified ocean to a two-layer scheme, it is important to make a correct estimation of ρ_1 and ρ_2. As a first iteration, the depth of the isopycnal surface of σ_θ=26.2, generally located in the center of the pycnocline, at each of the 52 stations was initially taken as

$h(x,y)$. Then, we defined $g'(x,y)$ at each station as the ratio of geopotential anomaly to anomaly of upper layer thickness:

$$g'(x,y)=(\Phi(x,y)-\Phi^*)/(h(x,y)-h^*), \quad (7)$$

with $\Phi^*=6.34$ m^2/s^2 and $h^*=95$ m as undisturbed parameters of the upper layer. Then (7) was inverted using a set of constant (i.e., independent of station location) values of g' in the range $g'=0.005$-0.035 m/s^2 to get the corrected values $h'(x,y)$ of the thickness of the upper layer. We found that the constant value of $g'=0.015$ m/s^2 corresponds to the minimum of the standard deviation

$$\delta h=\sqrt{\frac{1}{N}\sum_{i=1}^{N}(h_i-h'_i)^2} = 10$$

of the depth difference in meters between the two interfaces. The distribution of the calculated $h'(x,y)$ did not coincide exactly with the observed depth of the $\sigma_\theta=26.2$ isopycnal but was everywhere close to it and within the pycnocline. This value of g' was therefore accepted as the best approximation to the real stratification at all stations.

Substituting the values $h^*=95$ m, $g'=0.015$ m/s^2, $f_0=6.6*10^{-5}$ s^{-1} yields $L_R=18$ km and $\epsilon=5.5 \times 10^{-3}$. The distribution of dimensionless thickness $H(x,y)$ was calculated using (4). An initial data adjustment was undertaken to damp the small-scale noise in the potential vorticity field by running the model for a short time with an additional term for dissipation, implemented in the form of a biharmonic friction operator $A\nabla^4 H$ on the right side of (3). This procedure effectively filtered out small scale noise and did not result in any visible distortion of the initial distribution of $H(x,y)$.

The initial distribution of $H(x,y)$ based on the "corrected" locations of the CTD stations occupied during the first survey is shown in Figure 7. The area outlined by dashes shows the region in which the model was run and for which results are shown in subsequent figures.

The evolving $H(x,y)$ field shows the translation of the modeled cyclonic eddy over a time interval of 5 days between

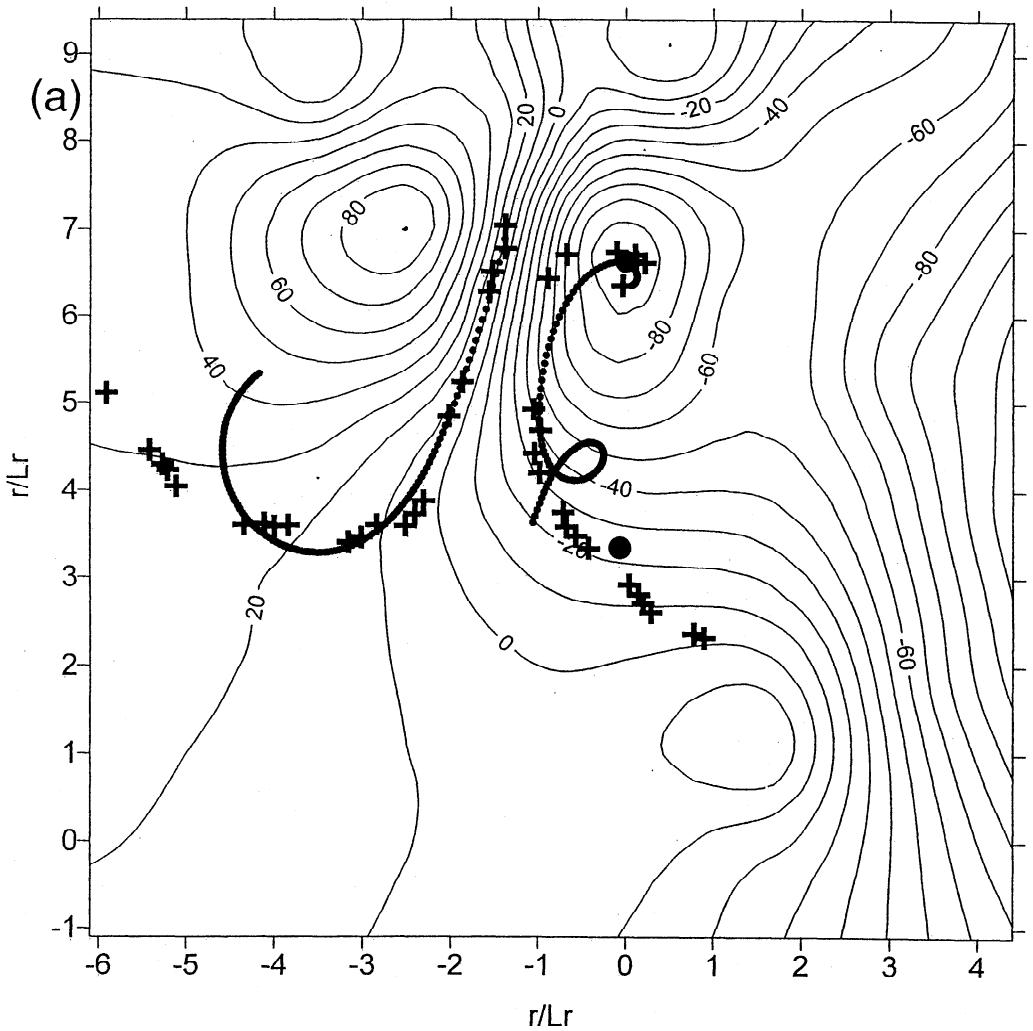

Figure 8. Distribution of $H(x,y)$ and drifter trajectories: (a) calculated at time = 0, and (b) - calculated at time = 5 days. The point with nondimensional coordinates (0, 0) is located at 26.30°N, 16.70°W. Locations of the eddy center during first and second surveys are shown by solid circles. Observed drifter trajectories (shown by pluses) are superimposed with computed trajectories of floats (shown by dots) released at the start time at the same points.

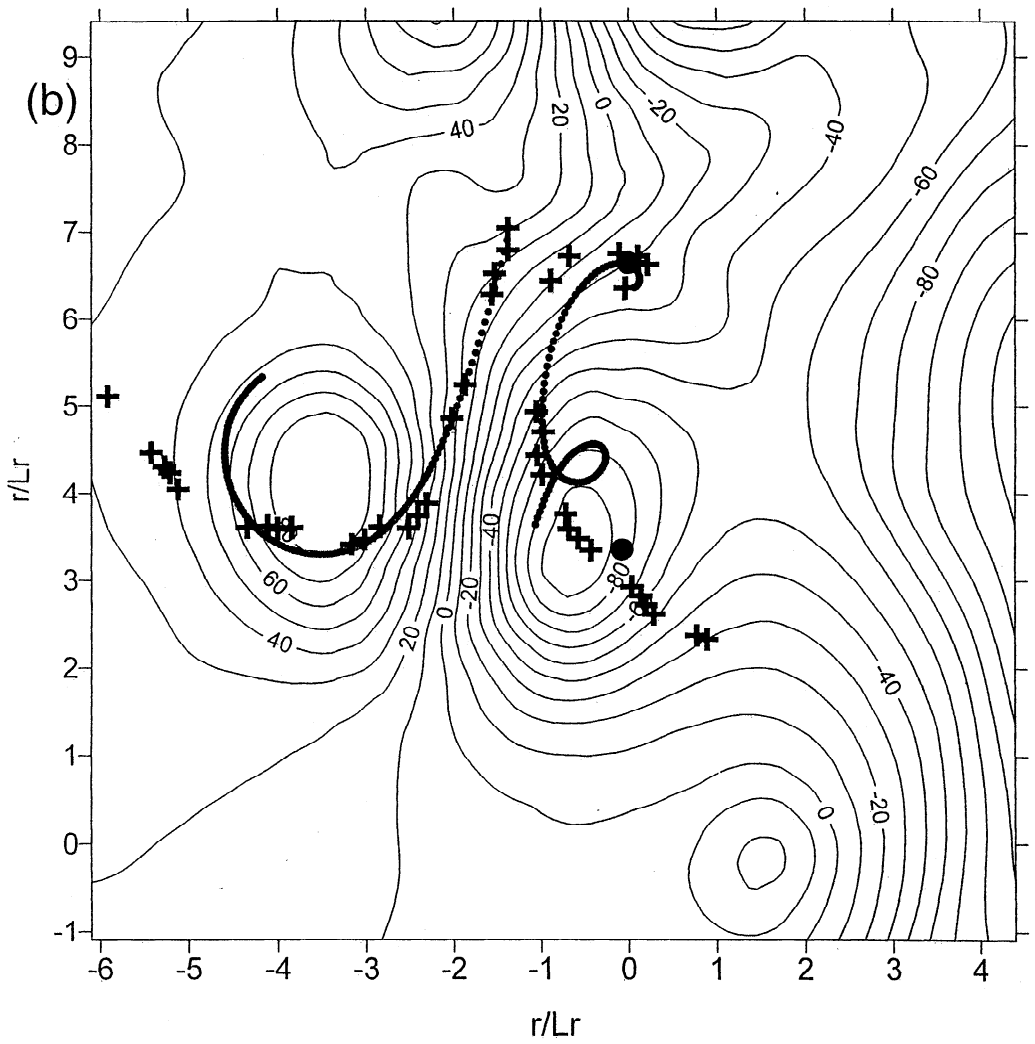

Figure 8. (continued)

the first and second surveys (Figure 8a and b). Numerical simulation gives an adequate prediction of the main parameters of the Eulerian motion of the cyclonic eddy: the distance and direction of displacement, the spatial scale and the intensity of the eddy at its final position. According to satellite images, the adjacent anticyclonic eddy is a stable feature trapped behind the island of Tenerife and, in contrast to our results, does not move significantly. We can not consider its dynamics in any detail because of the lack of CTD data in and around this structure.

The observed drifter trajectories (shown by pluses at the Argos fixes) are superimposed on the initial and final fields of H in Figure 8. The computed trajectories of model floats released at time t=0 at the launch positions of the real drifters are shown by circles. The observed trajectories show a strong divergence in their track. Float K was initially carried in the strong flow between cyclonic and anticyclonic eddies toward the southwest and then around the anticyclone. The computed trajectory of this float gives a good approximation of the observed one until about the fourth day. At that time the observed and predicted trajectories diverged. This is most likely due to the poor observational knowledge of the flow field in the southwest of the area, where the field is largely extrapolated (see Figure 7 for the observation points).

Float R was launched close to the center of the cyclonic eddy but spiralled outwards as it moved around the eddy and southwards with the background drift (Figure 8). The predicted trajectory followed a similar overall path but was quite different in detail. The prediction showed a complete revolution of the eddy after about 3 days and indicated a shorter overall translation. Small variations in the initial release position within the eddy of the simulated drifter showed little difference in predicted trajectory. The discrepancies between actual and simulated trajectories are most probably the result of the lack of definition of the flow field as the simulated drifter moves outside the area initially sampled and also due to temporal changes in the distribution during the 5-day drift. As shown below, in regions of strong background shear the trajectories are sensitive to even small differences in the shear.

To demonstrate this sensitivity of the Lagrangian characteristics to small changes in background flow, we generated six different versions of distribution of $H(x,y)$ using different parameters for interpolation of the observational data. This procedure did not change the Eulerian fields appreciably, but resulted in small variations of thickness (±5 m) of the active layer $h(x,y)$ and small changes of background shear flow between the eddies (Figure 9). The model was run for 5 days in all experiments. At the start of each one, six simulated

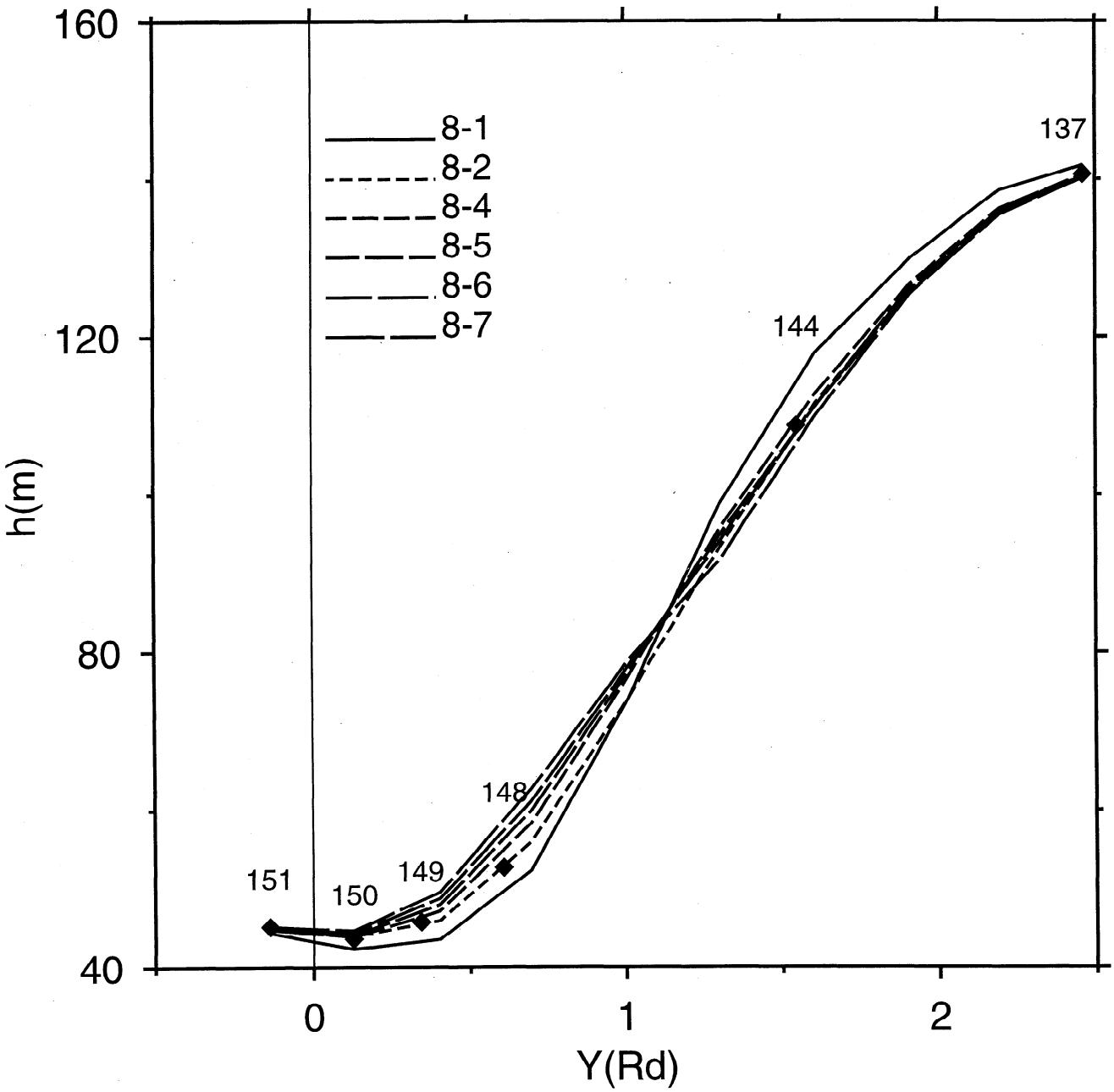

Figure 9. Variations of the active layer thickness $h(x,y)$ along the line between St.151 (center of the cyclonic eddy) and St.137 (anticyclonic eddy) due to different interpolation schemes for observational data. Values of h at CTD stations are shown by pluses.

floats were released at fixed points in the strong shear zone between the eddies. Their trajectories were computed and overlaid on the final Eulerian fields.

The results, shown in Figures 10a to 10f, confirm that the trajectories of floats are indeed sensitive to small changes in the initial distribution of $H(x,y)$. Although released at the same points, floats in different numerical experiments demonstrate significantly different Lagrangian characteristics, whereas the Eulerian characteristics change by practically undetectable amounts. The sensitivity and accuracy of the numerical scheme was tested by running the model at different time and space steps and by checking the conservation of potential vorticity along the float trajectory. The experiments showed little difference in the final distributions of h and q, and small difference in float trajectories when the time step was changed from $\Delta t = 1.32 \times 10^{-3}$ to 0.66×10^{-3} and space step from $\Delta x =$ 0.3 to 0.4. The standard deviation of potential vorticity at the float location resulting from numerical noise was between σ_q=6 and σ_q =13 (in nondimensional units) for different floats, which is much smaller than the reference difference $\Delta q = 300$ between values of potential vorticity anomaly at adjacent stations 144 and 148. Hence the sensitivity of the modeling results to the changes of numerical scheme parameters was much less than that of uncertainties in the observational data, which demonstrates the numerical scheme is adequate for the situation. The obvious reason is that the numerical grid is

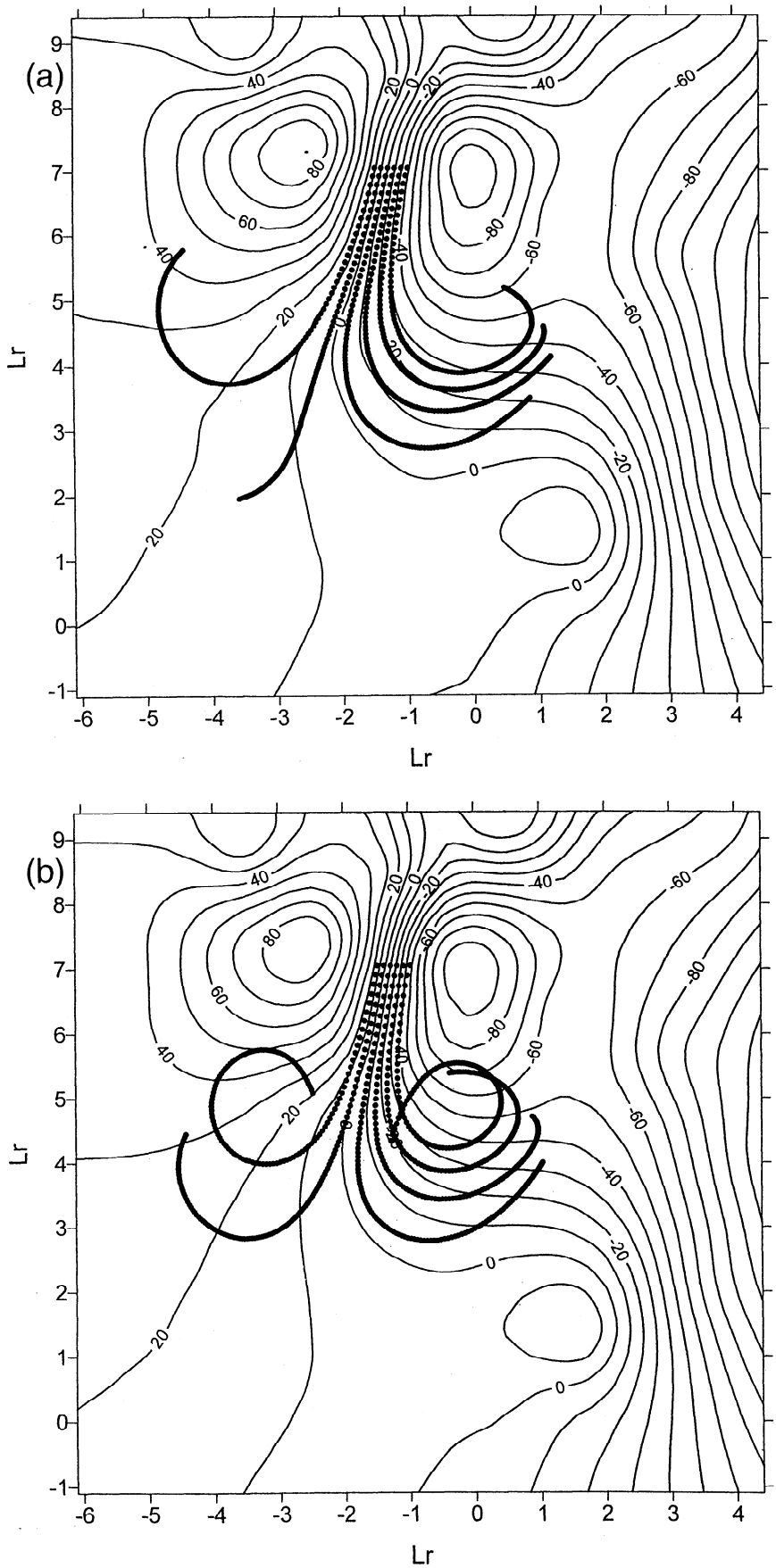

Figure 10. Computed trajectories of six floats released at the same locations for six slightly different initial distributions of $h(x,y)$. The only difference between the initial distribution is due to different interpolation between St.151 and St.137 (see Figure8). The difference between Lagrangian trajectories is much stronger: only one drifter turns right in Figure 10a, while four drifters turn right in Figure 10f.

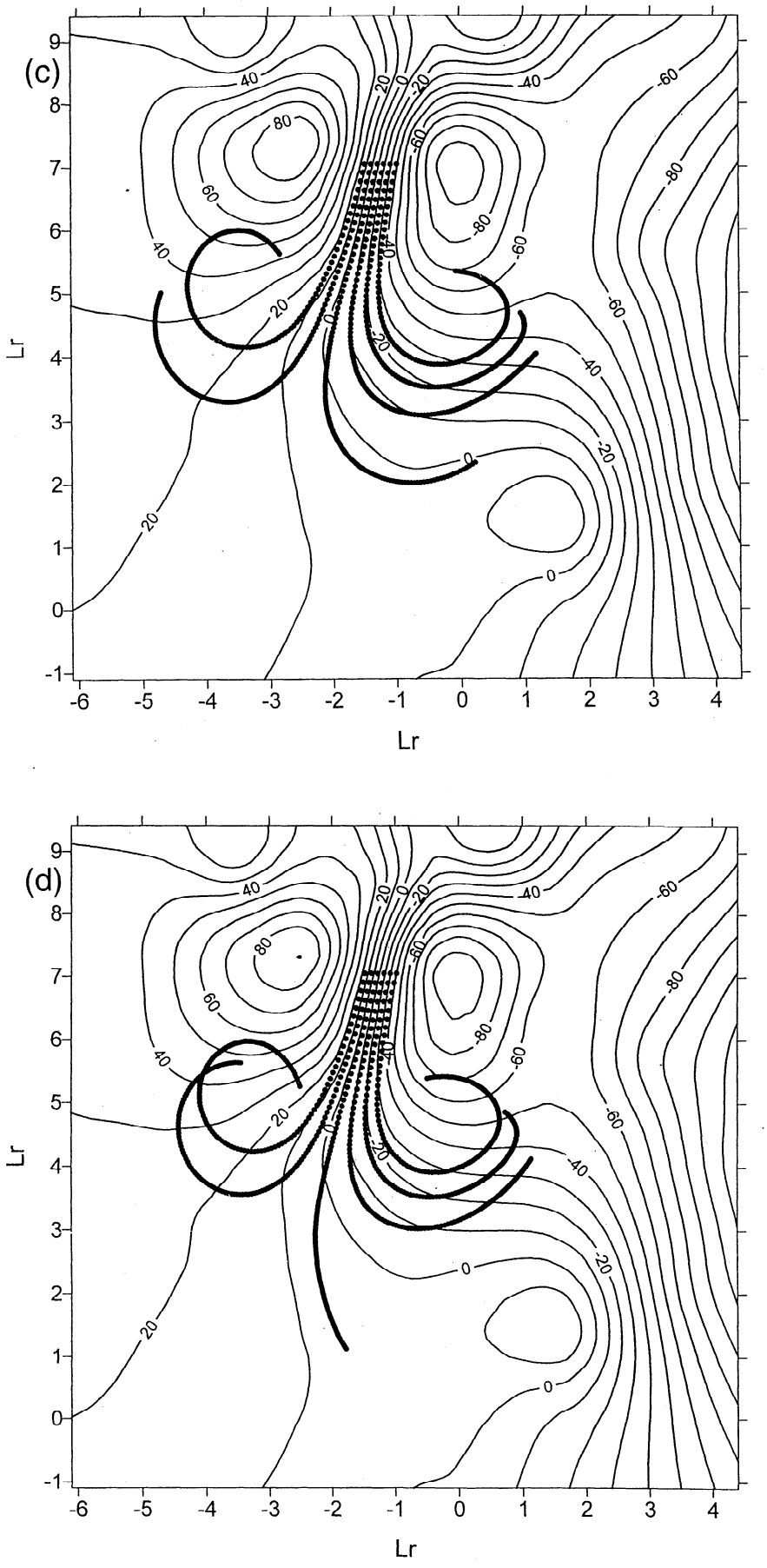

Figure 10. (continued)

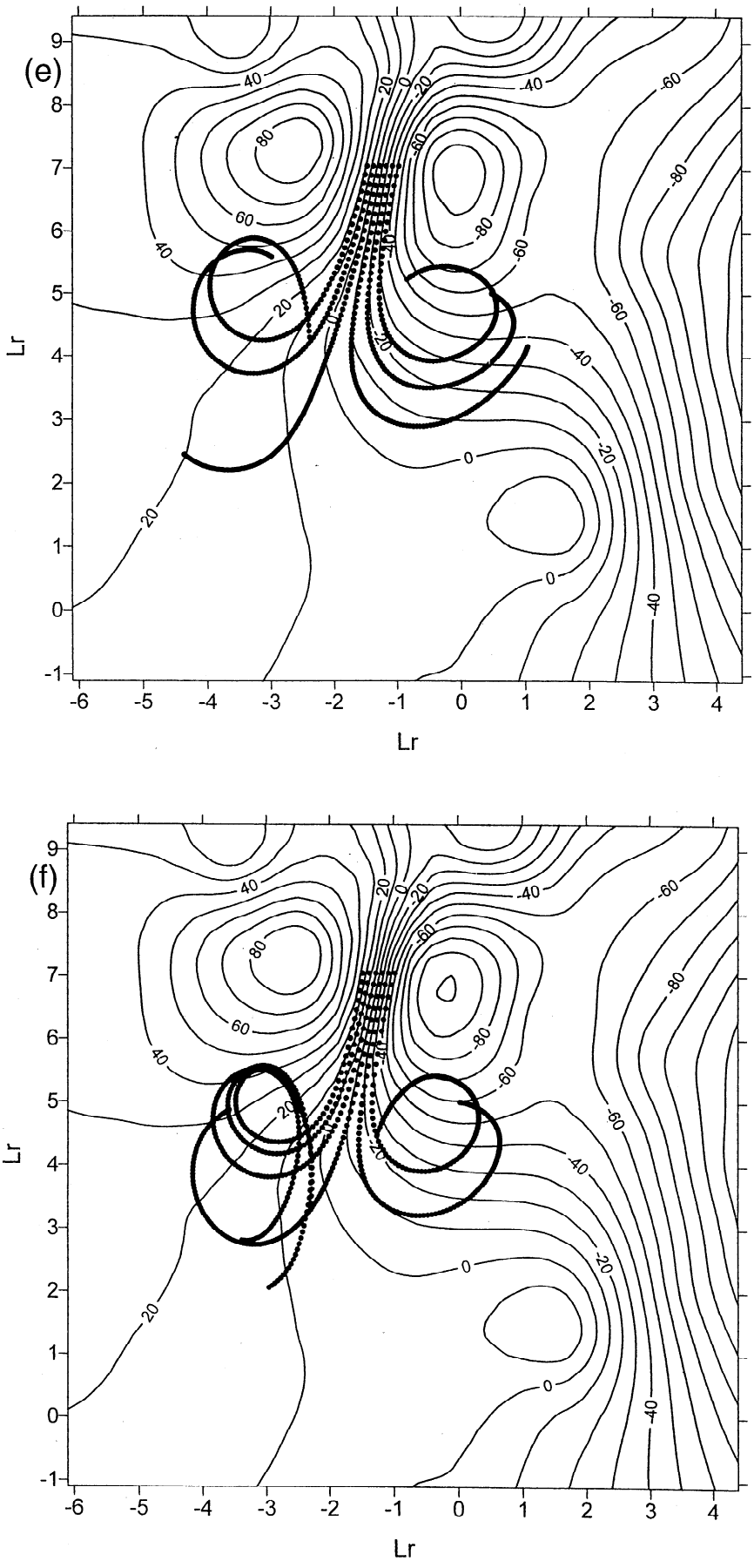

Figure 10. (continued)

much denser than the observational one. We conclude therefore that small changes in the dimensions of the trap zone of eddies caused by alteration of the background flow result in considerable changes of Lagrangian trajectories of the floats deployed near the Eulerian boundary of the eddy. This mechanism can be responsible for both trapping the floats by eddies as well as for allowing floats to escape from eddies, depending on the actual changes in the background flow.

5. Discussion and Conclusions

Drifters have been frequently observed apparently entering or leaving ocean eddies. In some cases these have been interpreted as drifters being incorporated at the formation stage of the eddy [*Bower et al.*, 1995]. In other cases, mechanisms such as time varying and rotating wind fields have been explored as possible causes [*Pingree and Le Cann*, 1991]. These authors showed that spiral displacement of drifters within an eddy can be induced by a circular, time-varying wind field which results in a radial velocity component. Another possibility for a float to spiral from the very eddy center is that if the eddy has a double core, the presence of a local surface jet current between cores could also result in spiral motion of the float. In the above cases, however, the flow field of the background and eddy, and their changes, were unknown because of lack of supporting data. For this reason the interpretations have a certain speculative element.

Even when supporting data are available, the method of calculation of geostrophic currents from the oceanographic data at CTD stations (Eulerian approach) suffers from several well-known disadvantages. First, it yields only relative currents with respect to an assumed reference level. Second, it provides averaged values between stations usually 10 or more kilometers apart which do not provide information on small-scale variations significant to the Lagrangian characteristics of currents. If an eddy is tracked with one drifter, the fact that the looping motion of the drifter ends abruptly does not necessarily mean that the eddy has disappeared. The eddy may persist, but its trap zone may have been reduced by changes in the background flow, so releasing the drifter from the eddy. Conversely, the observation that a drifter moving downflow suddenly begins a looping motion does not always imply generation of a new eddy. The drifter might be trapped in the core of a preexisting eddy. This implies that during field experiments, clusters of drifters must be launched in an eddy in order to reveal its Lagrangian characteristics.

The results of the model show that drifters may be incorporated into or ejected from eddies independent of their sense of rotation due to a simple mechanism dependent on the temporal and spatial change in the surrounding flow conditions. It is possible therefore to explain observed buoy trajectories without resort to complicated wind forcing or invoking eddy generation or decay. The drifter behavior depends on its release position relative to the eddy trap zone and the relative strengths of the eddy and the changing background flow. As the eddy experiences changing flow and shear, the trap zone can expand, so capturing nearby drifters, or contract so releasing previously trapped drifters.

This mechanism alone cannot, of course, explain all aspects of drifter behavior near eddies. The simple two-layer model used here has taken no account of wind forcing, or of any inherent convergent or divergent motions within eddies, due, for example, to frictional circulations. These motions must be combined with the particle motions demonstrated here to obtain a complete description of the flow field associated with any eddy. Nevertheless, we believe that the proposed mechanism is one which characterizes many features of motion in relation to eddies that have been observed up to now. In practice, a precise prediction of particle trajectories is likely to require a more detailed knowledge of the background shear than is generally available. The difficulties of interpretation of single drifter tracks in the absence of supporting background information are clear.

Acknowledgments. This work was carried out partially during the visits to the School of Ocean Sciences, University of Wales Bangor by G. I. Shapiro and S. L. Meschanov with funding by the Russian Foundation of Basic Research grant 94-05-17302, the Royal Society - Russian Academy of Sciences Exchange Programme, and the Sir Kirby Laing Fellowship. Financial support for the field observations was provided with funds from the European Community MAST-1 project 0031 and the Spanish Comisión Interministerial de Ciencia y Tecnología (CICYT). We are grateful to our many colleagues who participated in making the field observations.

References

Arístegui, J., P. Sangrá, S. Hernández-León, M. Cantón, A. Hernández-Guerra, and J.L. Kerling, Island-induced eddies in the Canary Islands, *Deep Sea Res.*, *41*(10), 1509-1526, 1994.

Arístegui, J., et al., The influence of island-generated eddies on chlorophyll distribution: A case study around Gran Canaria, *Deep Sea Res.*, *44*(1), 71-96 , 1997.

Bower, A.S., L. Armi and I. Ambar, Direct evidence of meddy formation off the southwestern coast of Portugal, *Deep Sea Res.*, *42*(9), 1621-1630, 1995.

Cheney, R.E., P.L. Richardson and K. Nagasaka, Tracking a Kuroshio cold ring with a free-drifting surface buoy, *Deep Sea Res.*, *27*(2), 641-654, 1980.

Dewar, W.K., and G.R.Flierl, Particle trajectories and simple models of transport in coherent vorticities, *Dyn. Atmos. Oceans*, *9*, 215-252, 1985.

Flierl, G., Particle motion in large-amplitude wave fields, *Geophys. Astrophys. Fluid Dyn*, *18*, 39-74., 1979.

Gründlingh, M.L., Drift of a satellite-tracked buoy in the southern Agulhas Current and Agulhas Return Current, *Deep Sea Res.*, *25*, 1209-1224 , 1978.

Holloway, G., S.C. Riser, and D.Ramsden, Tracer Anomaly evolution in the flow field of an isolated eddy, *Dyn. Atmos. Oceans*, 10, 165-184, 1986.

Kirwan, A.D., Jr., Notes on the cluster method for interpreting relative motions, *J. Geophys. Res.*, *93*(C8), 9337-9339 , 1988.

Kirwan, A.D., G. McNally, M.S. Chang and R. Molinari, The effect of wind and surface currents on drifters, *J. Phys. Oceanogr.*, *5*, 361-368 , 1975.

Larichev, V.D., and G.M. Reznik, Strongly non-linear, two-dimensional isolated Rossby waves, *Oceanology*, Engl. Transl., *16*, 547-550, 1976.

Maksimenko, N.A.,and O.I. Orlov, The integral characteristics of the quasistationary "Gaussian" eddy core in the homogeneous or shear flows (in Russian), *Okeanologiya, Moscow, 31*, 34-41, 1991.

Navarro Pérez, E., H.S. Velez Muñoz and K.A. Wild. Hesperides Cruise 9308 Report: Hydrographic fields, *Report 0031-16*, Sch. of Ocean Sci., Univ. of Wales, Bangor, 1994.

Pingree, R.D. and B. Le Cann, Drifting buoy in the field of flow of two eddies on East Thulean Rise (Northeast Atlantic), *J. Geophys. Res.*, *96* (C9), 16759-16777 , 1991.

Richardson, P.L., D. Walsh, L. Armi, M. Schröder and J.F. Price, Tracking three meddies with SOFAR floats, *J. Phys. Oceanogr.*, *19*(3), 371-383 , 1989.

Sanderson, B.G., Structure of an eddy measured with drifters, *J. Geophys. Res.*, *100* (C4), 6761-6776 , 1995.

Shapiro, G.I., Dynamics of isolated intrathermocline eddy,. *Oceanology*, Engl. Transl, *26*, 12-15., 1986.

Shapiro, G.I. and V.N. Konshin, On the evolution of intensive cyclonic-anticyclonic vortex pairs, in Mesoscale/Synoptic Coherent Structures in Geophys. Turbulence, Elsevier Oceanogr. Ser., 50,

edited by J.C.J. Nihoul and B.M. Jamart (Editors), Elsevier, New York, 1989.

Schultz Tokos, K.L., H.-H. Hinrichsen and W. Zenk, Merging and migration of two meddies, *J. Phys. Oceanogr., 24*, 2129-2141 , 1994.

Williams, G.P., Geostrophic regimes on a sphere and a beta-plane, *J. Atmos. Sci., 42*, 1237-1243, 1985.

Zenk, W., K.L. Schultz Tokos, O. Boebel, New observations of meddy movement south of the Tejo plateau, *Geophys. Res. Letters, 19*, 2389-2392, 1992.

E.D.Barton, School of Ocean Sciences, University College of North Wales, Menai Bridge, Anglesey LL59 5EY, Wales. (e-mail: oss041@sos.bangor.ac.uk)

S.L.Meschanov and G.I.Shapiro, P. P. Shirshov Institute of Oceanology, Russian Academy of Sciences, 23 Krasikova St., 117218 Moscow, Russia.

(Received July 5, 1996; revised April 10, 1997;
accepted June 16, 1997)